

MICROSTRUCTURAL INVESTIGATION OF NEW POLYTYPES OF PARISITE-(Ce) BY HIGH-RESOLUTION TRANSMISSION ELECTRON MICROSCOPY

DAWEI MENG[§], XIULING WU AND TAO MOU

Test Center, China University of Geosciences, Wuhan, 430074, People's Republic of China

DOUXING LI

*Laboratory of Atomic Imaging of Solids, Institute of Metal Research, Academia Sinica,
Shenyang, 110015, People's Republic of China*

ABSTRACT

Five new polytypes of parisite-(Ce) $[\text{CaCe}_2(\text{CO}_3)_3\text{F}_2]$ from a rare-earth-mineral deposit within an aegirine-bearing granite pluton in Sichuan Province, southwestern China, were found by HRTEM: *6R*₂, *8H*, *14H*, *36R* and *42R*. These new polytypes are all long-period ordered stacking structures, which may result from the distribution and the periodic variation in orientation of $[\text{CO}_3]$ groups between the unit layers of parisite-(Ce). The observed microstructures may be affected by the rock-forming environment. These new polytypes coexist with the very common polytype *6R*₁, disordered stacking series, and mixed-layer structures developed in the host polytype, *6R*₁.

Keywords: parisite-(Ce), polytype, high-resolution transmission electron microscopy, aegirine granite, Sichuan Province, China.

SOMMAIRE

Nous avons découvert cinq nouveaux polytypes de parisite-(Ce) $[\text{CaCe}_2(\text{CO}_3)_3\text{F}_2]$, *6R*₂, *8H*, *14H*, *36R* et *42R*, dans un gisement de terres rares associé à un pluton de granite à aegirine de la province de Sichuan, dans le sud-ouest de la Chine, suite à un examen en microscopie électronique par transmission à haute résolution. Tous ces polytypes ont une longue périodicité. La mise en ordre dans leur séquence d'empilement pourrait résulter de la distribution et la variation de l'orientation des groupes de $[\text{CO}_3]$ entre les couches de la structure de la parisite-(Ce). Les microstructures observées pourraient avoir été affectées par le milieu de croissance. Ces nouveaux polytypes coexistent avec le polytype courant *6R*₁, des séries d'empilement désordonné, et des mélanges de polytypes présents dans le polytype hôte, *6R*₁.

(Traduit par la Rédaction)

Mots-clés: parisite-(Ce), polytype, microscopie électronique par transmission à haute résolution, granite à aegirine, province de Sichuan, Chine.

INTRODUCTION

There are four mineral species in the calcium – rare-earth-element (Ca-REE, cerium-dominant) fluoro-carbonate mineral series: bastnäsite-(Ce) $[\text{Ce}(\text{CO}_3)\text{F}]$, parisite-(Ce) $[\text{CaCe}_2(\text{CO}_3)_3\text{F}_2]$, röntgenite-(Ce) $[\text{Ca}_2\text{Ce}_3(\text{CO}_3)_5\text{F}_3]$ and synchysite-(Ce) $[\text{CaCe}(\text{CO}_3)_2\text{F}]$. Donnay & Donnay (1953) and Van Landuyt & Amelinckx (1975) studied the structural characteristics of the bastnäsite and synchysite by X-ray diffraction and transmission electron microscopy (TEM). They considered bastnäsite-(Ce) and synchysite-(Ce) as two end-

members, and the other minerals as ordered mixtures of unit-layers of bastnäsite (B layer) and synchysite (S layer) stacked along the *c* direction. For example, parisite can be regarded as BS, and röntgenite as BS₂.

The structures of members of this series can be described in terms of four layers parallel to (0001): a CeF structural layer (*d*), a layer of CO₃ groups between two CeF layers (*e*), a layer of Ca (*f*), and a layer of CO₃ groups between calcium and CeF layers (*g*). The stacking sequences of bastnäsite-(Ce) (B), parisite-(Ce) (BS), röntgenite-(Ce) (BS₂) and synchysite-(Ce) (S) can be represented as *de*, *dedgfg*, *dedgfgdgfg* and *dgfg* respec-

[§] E-mail address: dwmeng@cug.edu.cn

tively (Van Landuyt & Amelinckx 1975). Details of the atomic arrangements in bastnäsite-(Ce) (Ni *et al.* 1993), synchysite-(Ce) (Wang *et al.* 1994) and synchysite-(Y) [YCa(CO₃)₂F] (Wang & Zhou 1995) have now been established. According to recent studies, thirty-two B_mS_n-type ($m \geq n$) new mixed-layer compounds and polytypes have been observed (Van Landuyt & Amelinckx 1975, Meng *et al.* 1995, 1996, 1997, 2001, Wu *et al.* 1997, 1998a, b, 2000). The formulae of these mixed-layer compounds can be expressed as $(m+n)\text{Ce}(\text{CO}_3)_m\text{F}_n\text{CaCO}_3$ ($m \geq n$). Here we report the characteristics of five new long-period polytypes of parisite-(Ce), 6R₂, 8H, 14H, 36R and 42R, as established by selected-area electron-diffraction (SAED) and high-resolution transmission electron microscopy (HRTEM).

EXPERIMENTAL

The grains of parisite-(Ce) (0.08–0.2 mm in diameter) are from a producing rare-earth-mineral deposit within an aegirine-bearing granite pluton in Maoniuping County, Sichuan Province, southwestern China (Fig. 1). The grains were pulverized and suspended in absolute alcohol. A drop of suspension was put on a copper grid coated with a perforated carbon film, in turn coated with gold, and then examined at 200 kV with a JEOL-2000EX electron microscope equipped with a top-entry goniometer stage ($\pm 10^\circ$ tilt) and an ultra-high-resolution pole piece [C_S (spherical aberration) = 0.7 mm] with an interpretable point-resolution of 0.21 nm. Electron-diffraction patterns were observed at 120 kV on a Philips CM 12 ($\pm 45^\circ$ tilt, C_S = 2.0 mm) transmission electron microscope.

BACKGROUND INFORMATION

In parisite-(Ce), the heavy atoms Ce and Ca constitute rhombohedral planes, respectively, and lie vertically with respect to the trigonal or hexagonal axis, alternatively. The trigonal planes formed by the CO₃ groups lie between the CeF layers and Ca layers, so that the crystal structure of this mineral can be described in terms of two basic unit layers, *i.e.*, the CeF–CeF layer and Ca–CeF layer. The CO₃ layers with two different orientations lie between the CeF–CeF and Ca–CeF basic layers and constitute the parisite-(Ce) unit layers (BS) 1.413 nm high (CeF–CO₃–CeF–CO₃–Ca–CO₃). The ordered stacking of the unit layers along the *c* direction and the periodic variation in orientation of the [CO₃] groups result in complex polytypic structures. The crystal structure of parisite-(Ce) has not been determined completely because of its complexity.

THE 6R₁ POLYTYPE OF PARISITE-(Ce)

The intense [0001] diffraction maximum can be observed in SAED patterns of parisite-(Ce); some SAED patterns and HRTEM images with different orientations

were taken around this diffraction maximum. The distribution of the diffraction spots in the [1210] SAED pattern (Fig. 2) are: rhombohedral symmetry, $h-k+l = 3n$ ($n = 0, \pm 1, \pm 2, \dots$), $c = 1.413 \text{ nm} \times 6 = 8.478 \text{ nm}$, R3 or $R\bar{3}$ space group, in accordance with the reflection condition of the 6R₁ polytype. The projection position of the unit cell in the [1210] direction is marked on the HRTEM image (Fig. 2). The positions of the layers *d*, *e*, *f*, *g* and the unit layer *dedfg* (BS, $c'' = 1.413 \text{ nm}$) were obtained by the thickness of the different structural layers (Ni *et al.* 1993), the projection position and the spacing between the diffraction spots c''^* (000 18) and c'''^* (0006) along the c^* in the corresponding SAED patterns. The analyses of the SAED patterns and HRTEM images of the polytype parisite-(Ce)-6R₁ with different characteristic orientations are listed in Table 1.

THE 6R₂ POLYTYPE OF PARISITE-(Ce)

A new polytype of parisite-(Ce) was determined in this study. The characteristics of SAED patterns in some orientations are similar to those of the 6R₁ polytype, but different in other orientations. A series of SAED patterns were taken around the [0001] direction. Figure 3 shows the SAED patterns and the indices of the diffraction spots of zones [1210], [4510], [1100], [5410] and [2110]. The diffraction spots such as 0003, 0009 and 000 15 on Figure 3c are formed by more intense diffraction, and will disappear as the transmission beam moves away from [1100].

To get enough three-dimensional electron-diffraction information, the SAED pattern (Fig. 3c) of zone [1100] in the same sample was selected, and a series of SAED patterns were taken around the [1120] direction. Figure 4 displays the SAED patterns of zones [1100], [20 20 01], [11 11 01], [8801] and [7701]. From these five SAED patterns and the relevant angles, a two-dimensional reciprocal lattice plane vertical to zone [1120] was made, in accordance with the SAED pattern of [1120] (Fig. 4f). In Figures 3a, 3e and 4f, the diffraction spots lie in layers parallel to the c^* direction. The distribution of the spots in the $0, \pm 3, \pm 6, \dots (3n)$ layers are identical, but different in the $\pm 1, \pm 2, \pm 4, \dots (3n \pm 1)$ layers. Along c^* , there are five extinction spots between 0000 and 0006, and the corresponding interplane distance $d_{(0006)}$ is 1.413 nm, and the cell height is $1.413 \text{ nm} \times 6 = 8.478 \text{ nm}$. The spots lie in the form of a parallelogram in Figures 3a, 3b, 3d and 3e, a hexagon in Figure 3f and a centered rectangle in Figures 4b, 4c, 4d and 4e. From the above, we can conclude that the reflection conditions are: $hkil$, $h-k+l = 3n$ ($n = 0, \pm 1, \pm 2, \dots$); $hh2hl$, $l = 3n$, and the possible space-groups are R3c and $R\bar{3}c$. The polytype can be described as 6R₂, a new polytype with rhombohedral symmetry. It can be seen by comparing the SAED patterns of the polytypes 6R₁ and 6R₂ that in the a^*c^* plane, the distribution spacing of the spots in the $3n \pm 1$ ($n = 0, \pm 1, \pm 2, \dots$) layers par-

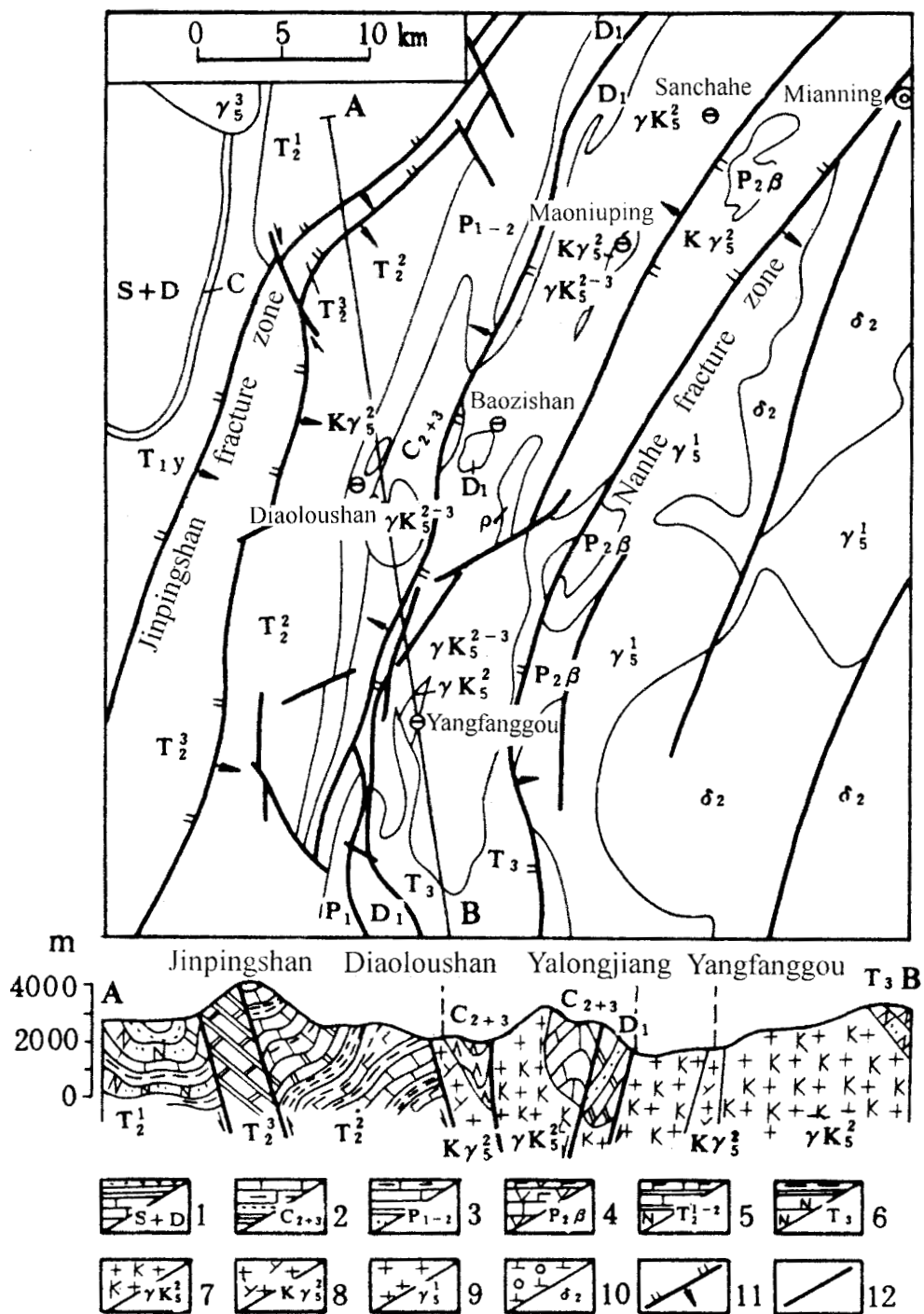


FIG. 1. The tectonic map of west Mianning (Li *et al.* 1992). Units: 1. Limestone, siltite and slate. 2. Crystalline limestone and metamorphic sandstone. 3. Limestone, argillite and basalt. 4. Basalt, andesite and crystalline limestone. 5. Siltite, greenschist, slate and marble. 6. Feldspar-dominant and quartz-dominant sandstone, and carbonaceous slate. 7. Moyite. 8. Aegirine-bearing granite. 9. Granite. 10. Diorite and quartz diorite. 11. Reverse fault. 12. Unspecified type of fault.

TABLE 1. THE SIX POLYTYPES OF PARISITE-(Ce)

Polytype	Cell and subcell (nm)				Number of unit layers (dedfgf)	Reflection conditions			Possible space-group
	a'	a	c'	c		hkl	$h\bar{h}0l$	$00l$	
$6R_1^*$	0.414	0.717	2.826 $c' = 6c''$	8.478 $c = 18c''$	6	$h-k+l = 3n$	$2h+l = 3n$	$l = 6n$	$R3, R\bar{3}$
$6R_2^{**}$	0.412	0.714	—	8.478 $c = 18c''$	6	$h-k+l = 3n$	$-h+l = 3n$ $l = 2n$	$l = 6n$	$R3c, R\bar{3}c$
$8H^{**}$	0.416	0.720	—	11.304 $c = 24c''$	8	—	—	$l = 8n$	$P6_3/mmc,$ $P6_3mc,$ $P6_2c$
$14H^{**}$	0.412	0.713	—	19.782 $c = 42c''$	14	—	—	$l = 14n$	$P6_3/mmc,$ $P6_3mc,$ $P6_2c$
$36R^{**}$	0.415	0.719	16.956 $c' = 36c''$	50.868 $c = 108c''$	36	$-h+k+l = 3n$	$h+l = 3n$	$l = 36n$	$R3, R\bar{3}$
$42R^{**}$	0.416	0.720	19.782 $c' = 42c''$	59.346 $c = 126c''$	42	$-h+k+l = 3n$	$h+l = 3n$	$l = 42n$	$R3, R\bar{3}$

Note: $a = a'\sqrt{3}$; H hexagonal, R rhombohedral; $c'' = 0.471$ nm, $c' = 1.413$ nm ($c' = 3c''$).

* known polytype; ** new polytype.

allel to the c direction is different, revealing their different symmetry, but identical in the $3n$ layers, proving that these two polytypes have the same subcell ($a'c''$, $a'c'$) and supercell (ac) (Table 1).

The SAED patterns and HRTEM images of the new polytype parisite-(Ce)- $6R_2$ corresponding to the crystal zones $[1210]$ and $[1100]$ (Fig. 5) reveal polytypic structures. Figure 5a shows the arrangement of the layers in the unit layer ($d = 1.413$ nm) of the polytype $6R_2$, the repeat period of the unit layers and the supercell size. It can be seen from the HRTEM images of the polytypes $6R_1$ and $6R_2$ that the arrangement and the orientation of the CO_3 structural layers between the unit layers are different, proving that these two polytypes possess a different symmetry.

POLYTYPES $8H$, $14H$, $36R$ AND $42R$ OF PARISITE-(Ce)

Different series of polytypes and the intergrowth structures (or syntactic growth among different polytypes) can be observed in single crystals of parisite-(Ce) from the Maoniuping County locality. These polytypes can be classified as types $2nH$ and $3nR$ (Figs. 5, 6, 7, 8, Table 1). The diffraction spots can be grouped into strong and weak spots. The distribution of the strong spots in the $3n$ layers is identical in each case, proving that these polytypes have the same hexagonal subcell $a'c''$ and $a'c'$ ($c' = 3c''$). The distribution and the spacing of the weak spots in the $3n \pm 1$ layers are different, proving that these polytypes have a different symmetry. The differences among the SAED patterns of the

parisite-(Ce) polytypes lie in the distribution of the weak spots (Fig. 8, Table 1).

In the SAED patterns of parisite-(Ce) polytypes $8H$ and $14H$, the spacing of the weak spots in the $3n \pm 1$ layers is eight times ($8H$, *i.e.*, seven extinction spots lie between the 0000 transmission spot and the 0008 diffraction spot) and fourteen times ($14H$, *i.e.*, thirteen extinction spots lie between 0000 and 000 14) that of the strong spots in the $3n$ layers, respectively. The corresponding analyses are shown in Figures 6, 7a and 8. The diffraction spots of the different zones of the polytypes $8H$ and $14H$ lie with hexagonal symmetry, *i.e.*, the supercell ac has a hexagonal symmetry. For example, the SAED patterns of $[12\bar{1}0]$ (Figs. 6a, 8d) display the strong spot (000 24) produced by the smallest subcell ($c'' = 0.471$ nm), the medium-strength spot (0008) produced by the subcell ($c' = c'' \times 3 = 1.413$ nm) and the weak spot produced by the supercell ($c = c'' \times 8 = 11.304$ nm). The corresponding HRTEM image (Fig. 6b) reveals the ordered periodic repeat of the stacked unit-layers (BS or *dedfgf*, $c'' = 1.413$ nm) in the new polytype parisite-(Ce)- $8H$ along the c direction. Each repeat period is made up of eight unit-layers (*dedfgf*), *i.e.*, the height of the supercell is $c = 1.413$ nm $\times 8 = 11.304$ nm, so the new polytype $8H$ is also called the 8-layer polytype.

The characteristics of the new polytypes $36R$ and $42R$ are: the smallest subcell ($a'c''$) and the subcell ($a'c'$, $a'c'$) have hexagonal symmetry, whereas the supercell (ac) has rhombohedral symmetry (Figs. 7, 8). The diffraction spots occur in accordance with the reflection

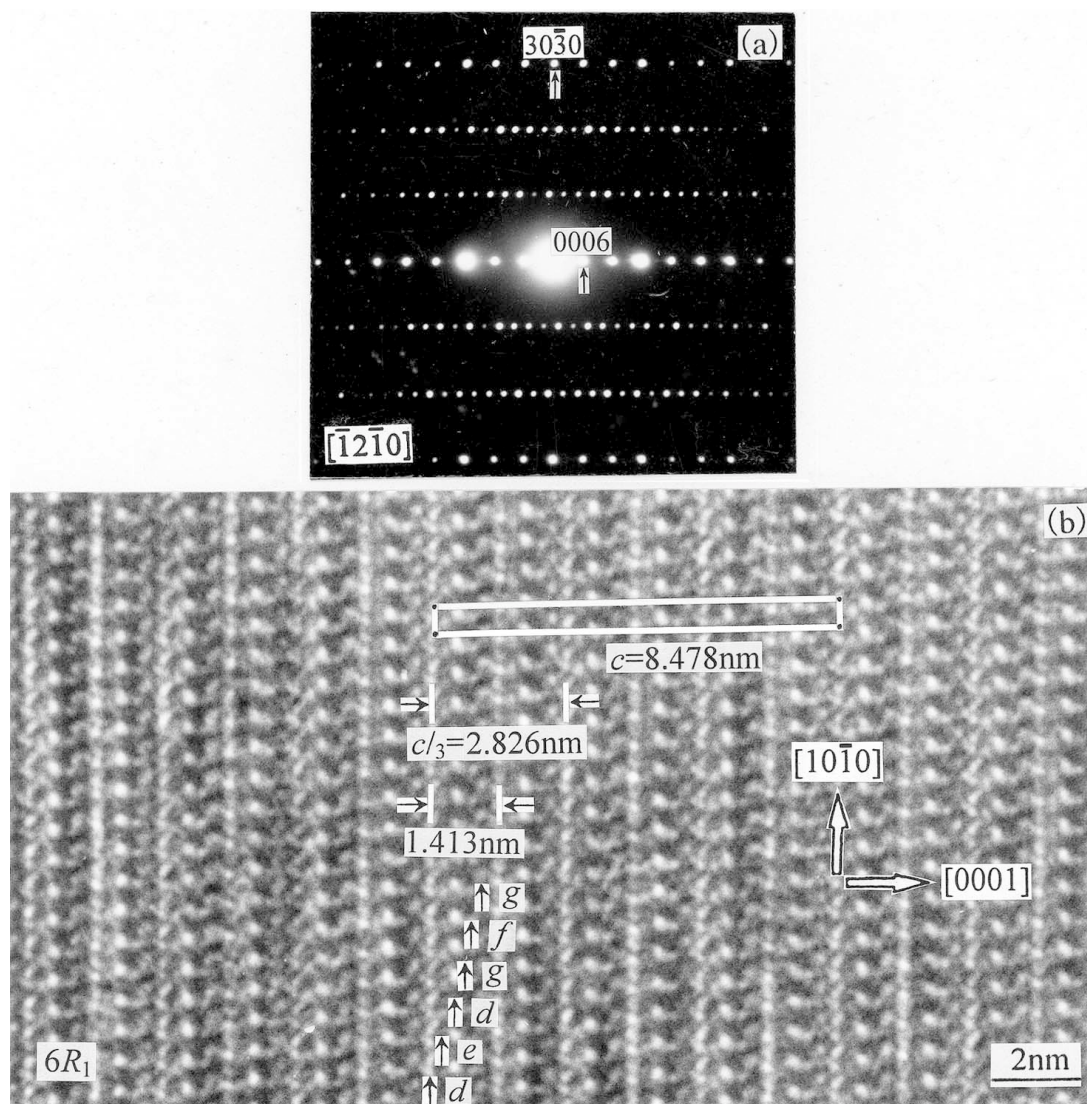


FIG. 2. SAED pattern (a) and HRTEM image (b) of the $6R_1$ polytype in parisite-(Ce) corresponding to the zone $[\bar{1}2\bar{1}0]$.

law $-h+k+l = 3n$ or $h-k+l = 3n$ ($n = 0, \pm 1, \pm 2, \dots$) (Table 1). In the SAED pattern of the polytype $36R$ corresponding to the zone $[\bar{1}2\bar{1}0]$, the spacing of the weak spots corresponding to rhombohedral symmetry in the $3n \pm 1$ layers is twelve times that of the strong spots in the $3n$ layers (Figs. 7b, 8c), so the nearest strong spot to the transmission spot along c^* was indexed as 000 36. This polytype was determined as a 36-layer polytype. The heights of the subcell and supercell of the new polytype parisite-(Ce)- $36R$ are $c' = 1.413 \text{ nm} \times 12 = 16.956 \text{ nm}$ and $c = c' \times 3 = 50.868 \text{ nm}$, respectively. A new polytype parisite-(Ce)- $42R$ (or 42-layer polytype)

was determined in the same way. The spacing of the weak spots in the $3n \pm 1$ layers is fourteen times that of the strong spots in the $3n$ layers, but there are forty-one reflection spots between 0000 and 000 42, so the polytype was determined as $42R$. In the different polytypes of parisite-(Ce), the distribution of the strong spots in the $3n$ layers is identical, showing that the unit layer and the subcell are identical in the different polytypes; the distribution, spacing and positions of the weak spots in the $3n \pm 1$ layers are different, reflecting the changes of the stacking period and the arrangement of the unit layers in the long-period stacking sequences.

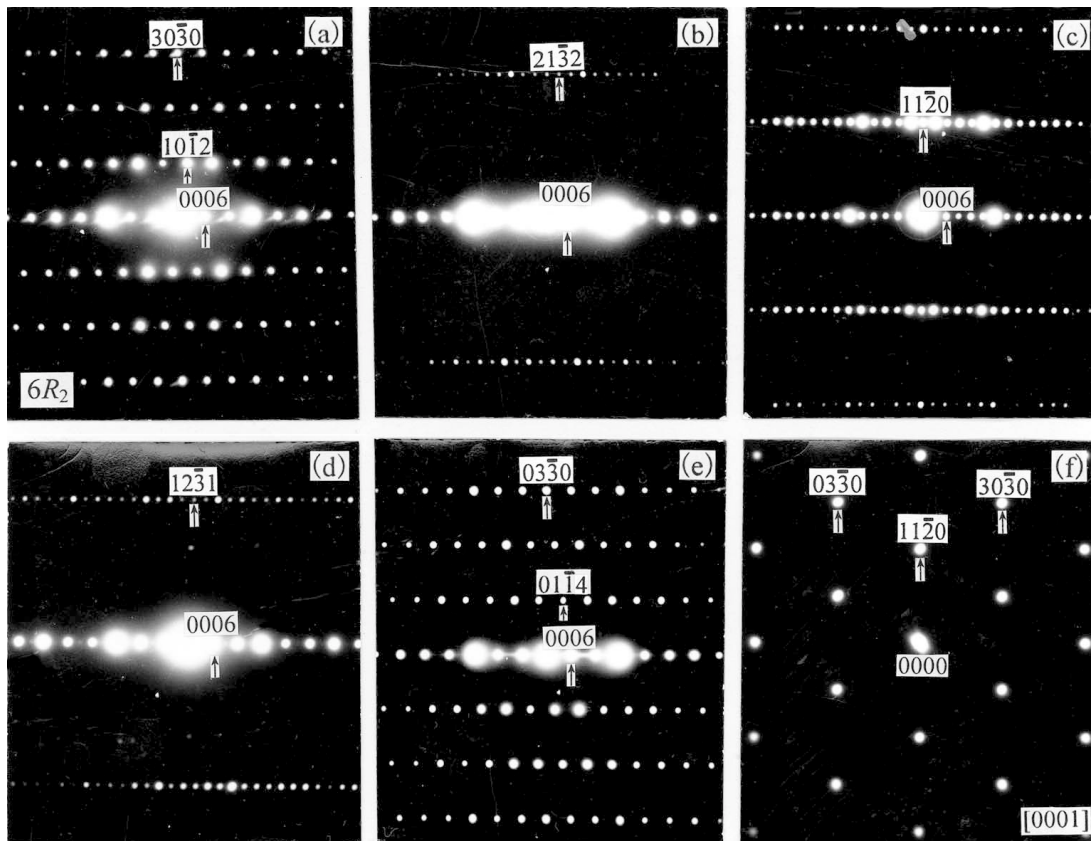


FIG. 3. a–e. SAED patterns of the $6R_2$ polytype obtained by tilting the crystal about $[0001]$. f. SAED pattern of the $6R_2$ polytype in parisite-(Ce) corresponding to the zone $[0001]$.

CONCLUSIONS

The results show that the polytypism of parisite-(Ce) is very complex. The most common polytype in nature is $6R_1$. Five new polytypes $6R_2$, $8H$, $14H$, $36R$ and $42R$ were determined. The six polytypes are all long-period ordered stacking structures; the cell sizes ($a = b = 0.713\text{--}0.720$ nm) are similar parallel to the unit layer (*dedfg*), whereas the range in cell height is $8.478\text{--}59.346$ nm, and the number of unit layers is between 6 and 42 (Fig. 8, Table 1). The five new polytypes are formed mainly because of the ordered stacking of the unit layers (*dedfg*) along the *c* direction, and the periodic changes in orientation of the $[\text{CO}_3]$ groups between the unit layers.

The diffraction spots appear in layers in the SAED patterns of different polytypes of parisite-(Ce) corresponding to the diagnostic zones (such as $[\bar{1}2\bar{1}0]$, $[2\bar{1}\bar{1}0]$ and $[1120]$). For different polytypes of parisite-(Ce), the distribution of the strong spots in the $3n$ layers are iden-

tical, whereas the distribution, spacing and positions of the weak spots in the $3n \pm 1$ layers differ. Among these six polytypes, $6R_1$ is most widespread, the five new polytypes are rare, and the long-period stacking polytypes ($8H$, $14H$, $36R$ and $42R$) are especially rare. The crystal grains ($0.2\text{--}0.8$ μm) of the five new polytypes coexist in the same natural crystal of parisite-(Ce) as the $6R_1$ polytype, disordered stacking sequences, mixed layer-structure by syntaxy, constituting the micro-polycrystal with local order and integral disorder. This assemblage may have been produced by hydrothermal activity during the cooling of the pluton (Zhang *et al.* 1998). The inhomogeneity of the structure reflects changes in the physicochemical environment, such as the rate of crystallization and of cooling. The polytypes of parisite-(Ce) result not only from the periodic changes of the unit layer stacking and the orientation of the $[\text{CO}_3]$ groups, but also from the variations of the conditions of formation such as the temperature, pressure, and medium of growth.

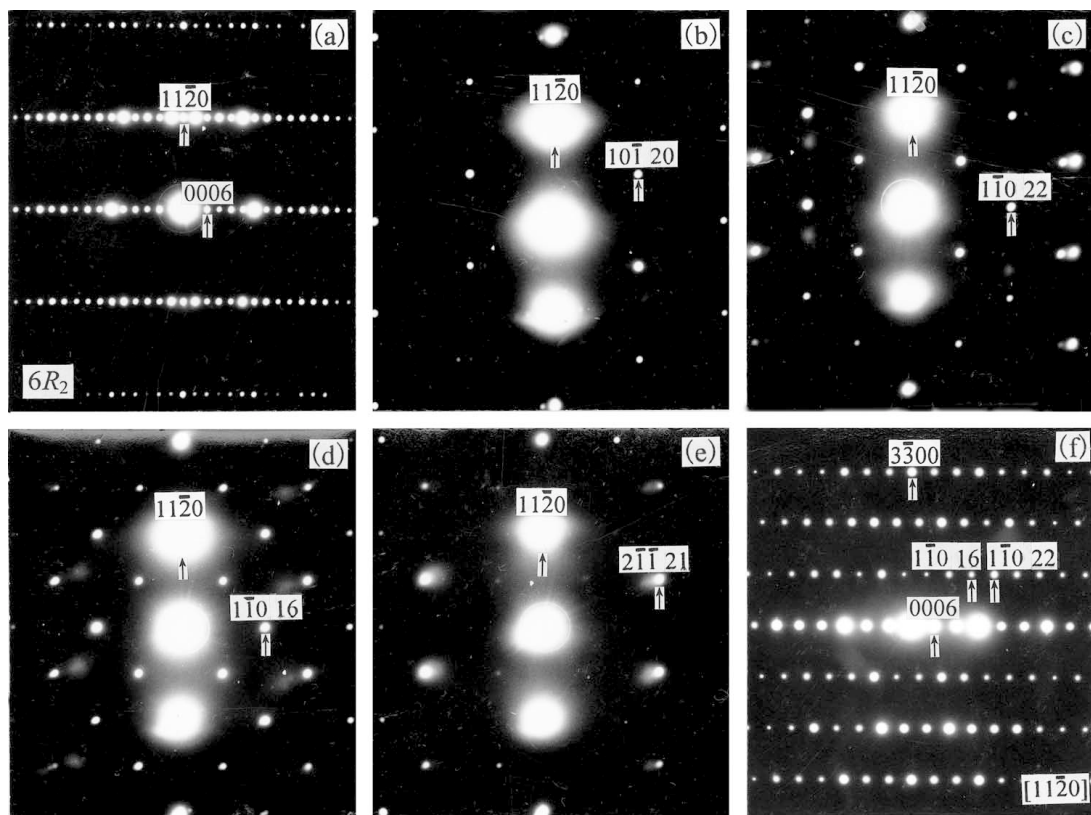


FIG. 4. a–e. SAED patterns of the $6R_2$ polytype obtained by tilting the crystal about $[11\bar{2}0]$. f. SAED pattern of the $6R_2$ polytype in parisite-(Ce) corresponding to the zone $[11\bar{2}0]$.

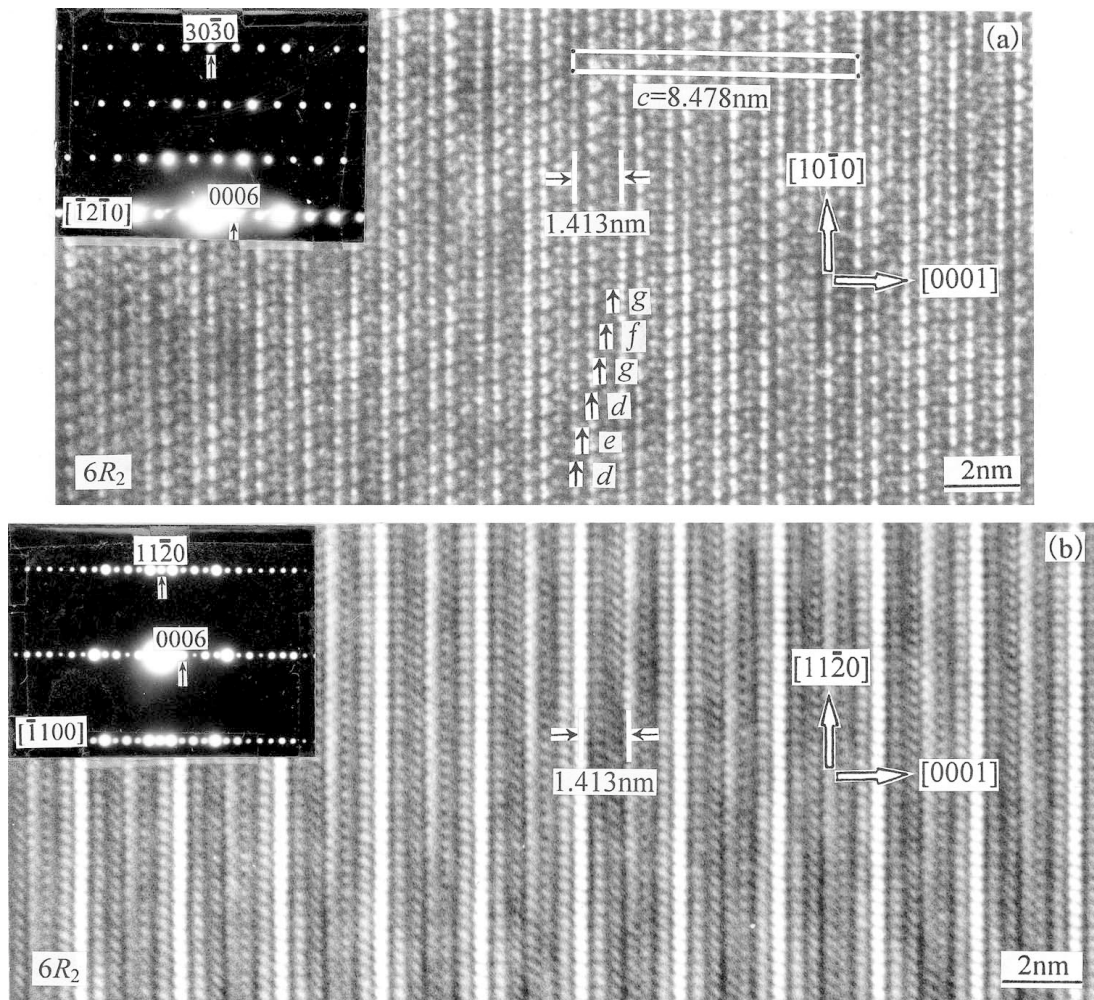


FIG. 5. a–b. SAED patterns and HRTEM images of the $6R_2$ polytype in parasite-(Ce) corresponding to the zones $[1\bar{2}\bar{1}0]$ and $[1\bar{1}00]$.

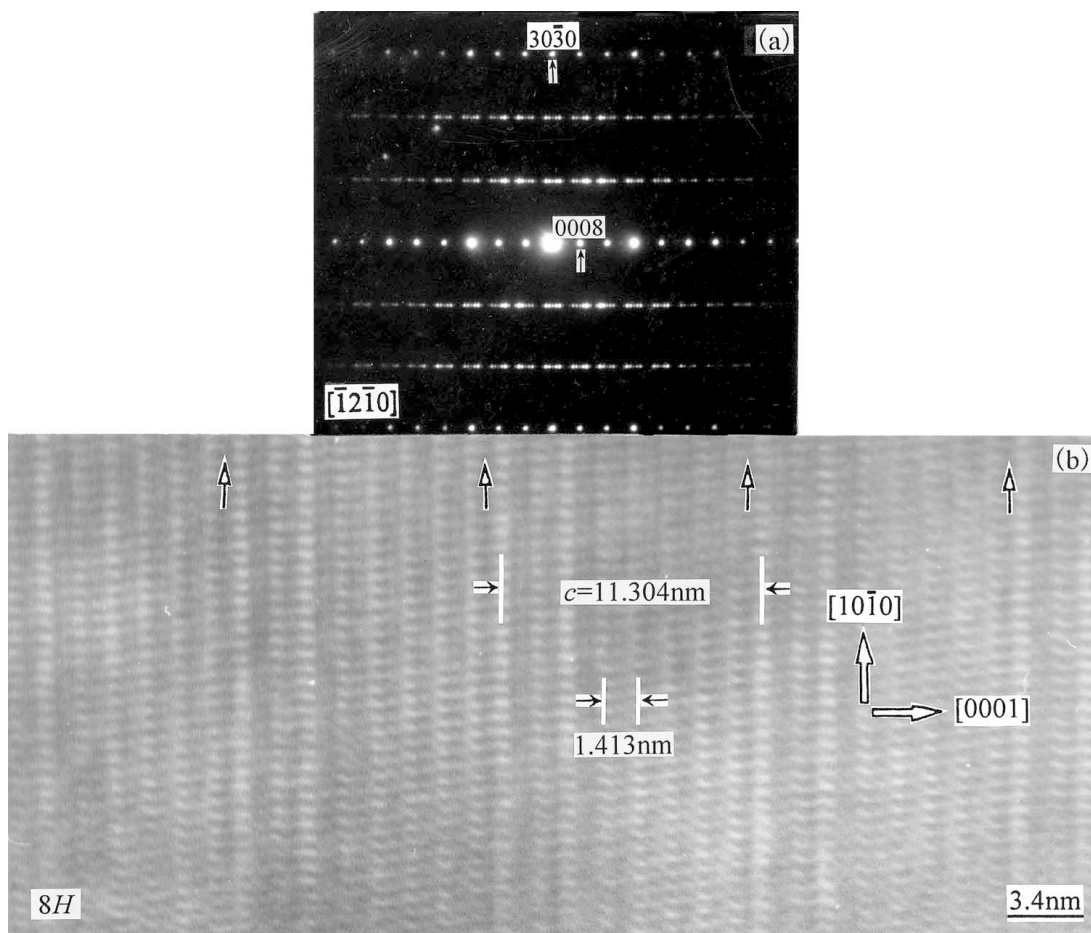


FIG. 6. a-b. SAED pattern and HRTEM image of the $8H$ polytypes in parisite-(Ce); the view is parallel to $[\bar{1}2\bar{1}0]$.

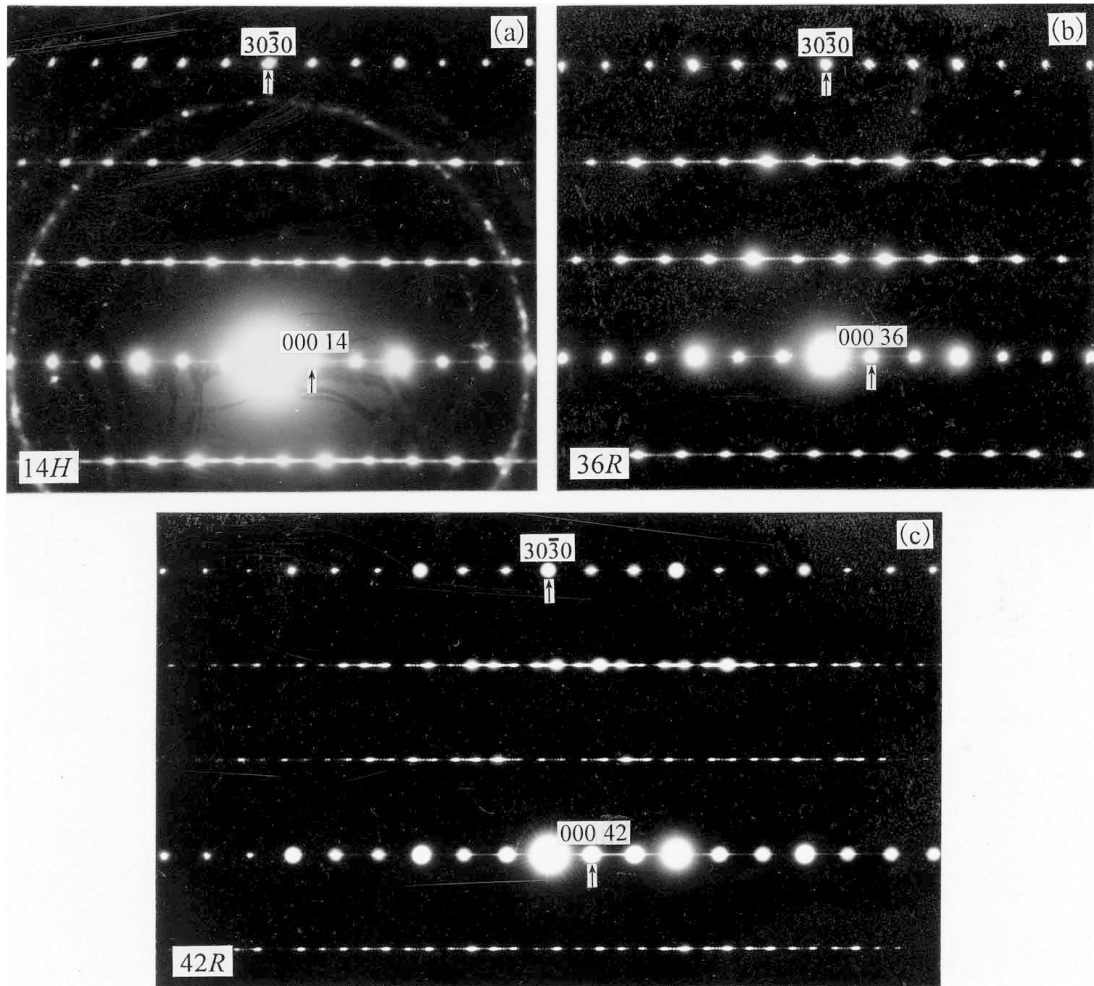


Fig. 7. a–c. SAED patterns of the $14H$, $36R$ and $42R$ polytypes in parisite-(Ce); the view is parallel to $[\bar{1}2\bar{1}0]$.

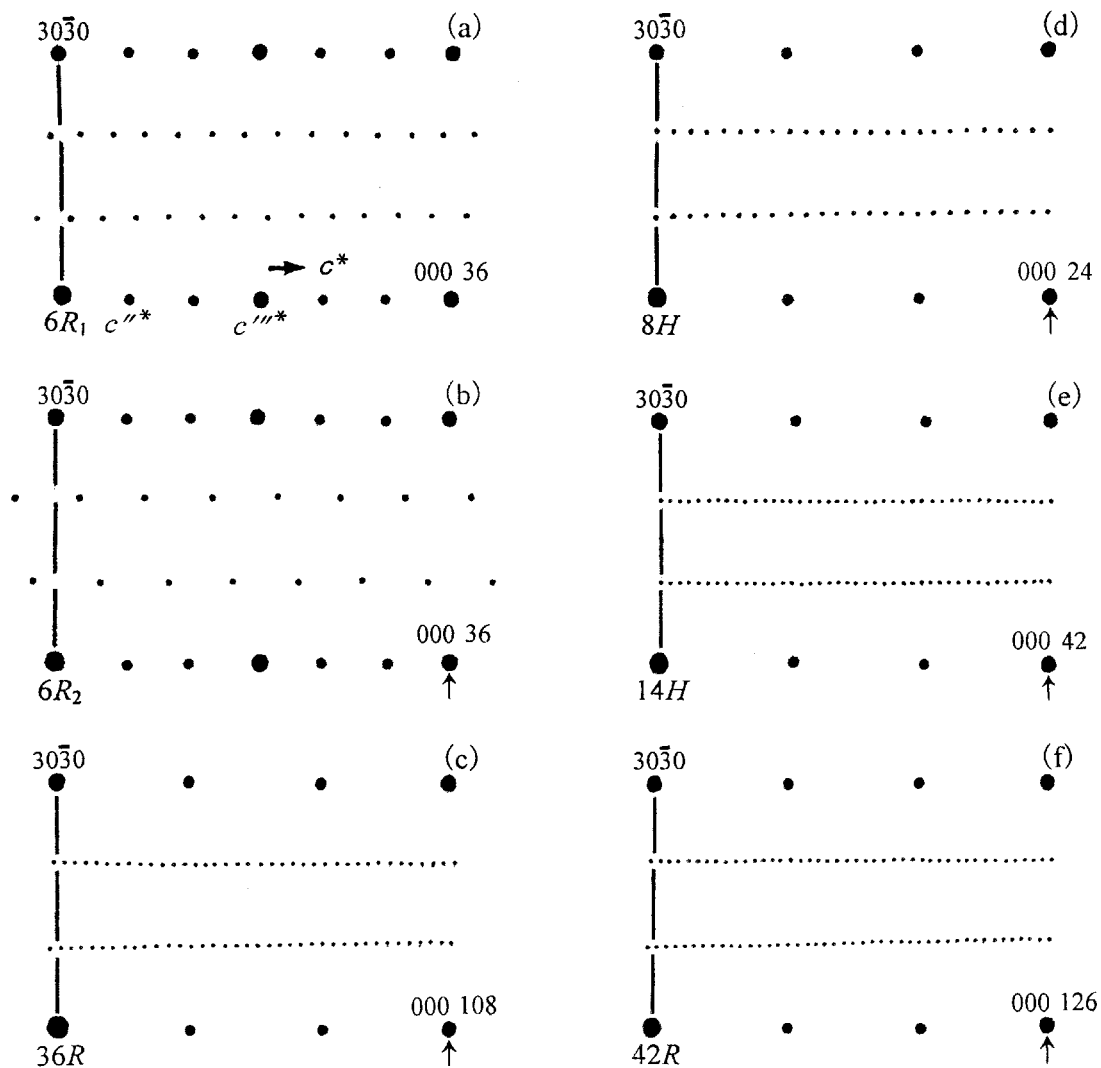


FIG. 8. Schematic representations of SAED patterns of the six polytypes in parisite-(Ce) corresponding to zone $[\bar{1}2\bar{1}0]$.

ACKNOWLEDGEMENTS

This project was supported by the National Natural Science Foundation of China (No. 49872069 and 40172019) and Foundation for University Key Teacher by the Ministry of Education of China (GG-709-10491-1008) and the Laboratory of Quantitative Prediction and Exploration Assessment of Mineral Resources by the National Land Resources Ministry, China. We acknowledge the helpful comments of the referees.

REFERENCES

- DONNAY, G. & DONNAY, J.D.H. (1953): The crystallography of bastnaesite-(Ce), parisite-(Ce), roentgenite-(Ce) and synchysite-(Ce). *Am. Mineral.* **38**, 932-963.
- LI, ZHONGLAI, JIANG, MINGQUAN & YANG, GUANGMING (1992): A newly discovered rare-earth metallogenic region and its prospect. *Geol. Sci. Technol. Information* **11**, 51-58 (in Chinese).
- MENG, DAWEI, WU, XIULING, MOU, TAO & LI, DOUXING (2001): Determination of six new polytypes in parisite-(Ce) by means of high resolution electron microscopy. *Mineral. Mag.* **65**, 797-806.
- _____, _____, PAN, ZHAOLU & YANG, GUANGMING (1996): HRTEM study of Ca-RE fluorocarbonate mineral series. *Proc. 30th Int. Geol. Congress (Beijing)* **2**, 499 (abstr.).
- _____, _____, _____, _____, LI, DOUXING & HU, KUIYI (1997): HRTEM study of three new regular mixed-layer structures in calcium-rare-earth fluorocarbonate minerals. *J. Chin. Rare Earth Soc.* **15**, 38-44.
- _____, _____, YANG, GUANGMING, PAN, ZHAOLU & LI, DOUXING (1995): TEM study of the microstructure in calcium-rare-earth fluorocarbonate minerals. *Proc. Eighth China-Japan Electron Microscopy Seminar*, 97-102.
- NI, YUNXIANG, HUGHES, J.M. & MARIANO, A.N. (1993): The atomic arrangement of bastnaesite-(Ce), Ce(CO₃)F, and structural elements of synchysite-(Ce), röntgenite-(Ce) and parisite-(Ce). *Am. Mineral.* **78**, 415-418.
- VAN LANDUYT, J. & AMELINCKX, S. (1975): Multiple beam direct lattice imaging of new mixed-layer compounds of the bastnaesite-synchysite series. *Am. Mineral.* **60**, 351-358.
- WANG, LIBEN, NI, YUNXIANG, HUGHES, J.M., BAYLISS, P. & DREXLER, J.W. (1994): The atomic arrangement of synchysite-(Ce), CeCaF(CO₃)₂. *Can. Mineral.* **32**, 865-871.
- _____, _____ & ZHOU, KANGJING (1995): The crystal structure of synchysite-(Y), YCa(CO₃)₂F. *Acta Petrol. Mineral.* **14**, 336-343 (in Chinese).
- WU, XIULING, MENG, DAWEI, LIANG, JUN & PAN, ZHAOLU (1997): Ordered-disordered stacking structure along the c-axis in calcium rare-earth fluorocarbonate minerals. *Proc. 30th Int. Geol. Congress (Beijing)* **16**, 49-57.
- _____, _____, MOU, TAO & PAN, ZHAOLU (2000): Domain structure in calcium-rare-earth fluorocarbonate minerals, Mianning County, Sichuan Province, China. *J. Chin. Rare Earth Soc.* **18**, 144-147.
- _____, _____, PAN, ZHAOLU, YANG, GUANGMING & LI, DOUXING (1998a): Transmission electron microscopic study of new, regular, mixed-layer structures in calcium-rare-earth fluorocarbonate minerals. *Mineral. Mag.* **62**, 55-64.
- _____, _____, YANG, GUANGMING, PAN, ZHAOLU, LI, DOUXING, DAI, JIYANG & HU, KUIYI (1998b): Syntactic intergrowth structure in the calcium-rare-earth fluorocarbonate minerals. *J. Chin. Rare Earth Soc.* **16**, 198-203.
- ZHANG, PEISHAN, TAO, KEJIE, YANG, ZHUMING & YANG, XUEMING (1998): *Rare Earth Mineralogy of China*. Scientific Publishing House, Beijing, China (in Chinese).

Received August 19, 2000, revised manuscript accepted September 30, 2001.